

1). Image performance

The window is very near to a focal plane, so imperfections in the window material will affect image quality. On the other hand, the beam size is quite small so that only a relatively small wavefront aberration will be introduced by a non-flat or non-parallel window.

There are several ways in which the window can introduce wavefront aberrations. One way is via manufacturing errors which could compromise flatness and parallelism of the window surfaces. It is very difficult to model surface error in Zemax, although Code V does have this facility. In any case, typical surface error on a window is likely to be much smaller than what we require. A non-parallel surface can be modeled as a wedge in Zemax, and typical manufacturing tolerances give no noticeable deterioration in image performance. Another source of wavefront aberrations comes from the fact that the window will flex under the pressure gradient across it causing surface deformation.

Window surface deformation might be important for NIRSPEC because the optics are nearly diffraction limited, and we cannot afford to introduce excess wavefront aberrations. Consider an example of a CaF₂ window having a 5 mm thickness. What will be the surface deformation? The IR Handbook (p. 7-102) gives an equation, reproduced below as equation 1, which can be used to calculate the sag, $w(\rho)$, versus normalized radial coordinate, ρ for a window.

$$w(\rho) = \frac{p a^4}{64 D} (1 - \rho^2) \left[\frac{5 + \gamma}{1 + \gamma} - \rho^2 \right]$$

where p = pressure differential,
 a = window radius,
 $D = E b^3 [12(1 - \gamma^2)]^{-1}$,
 E = Young's modulus,
 b = window thickness,
 γ = Poisson's ratio,
and ρ = normalized radial distance.

(1)

I have calculated the results for NIRSPEC assuming a variety of window thicknesses. The results are shown graphically in Figure 1. Here I give the "deformation," also known as the "sag," for window thicknesses from 2 to 10 mm. I have plotted this on a log scale, so it is somewhat difficult to imagine the shape of the window just by looking at the plots. To provide some insight, I have replotted the sag in Figure 2 for a window thickness of 7.5 mm, where I have also plotted the shape of a spherical surface with a best-fit radius. This best-fit radius is given by equation 2. The values used in equation 1 to generate Figure 2 are shown in Table 1.

$$r = \frac{a^2}{2 \text{ sag}}$$

where a = physical radius of clear aperture.

(2)

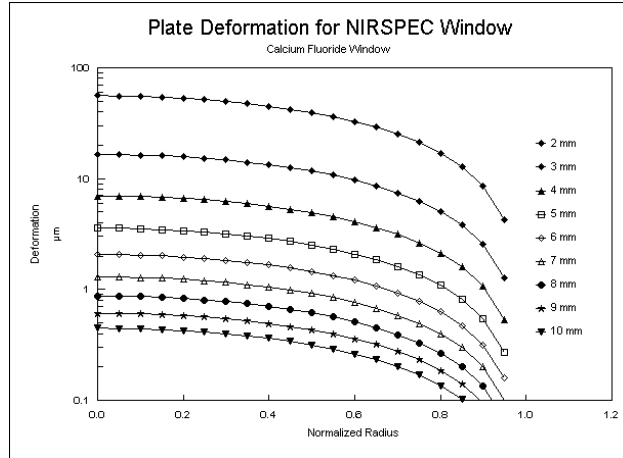


Figure 1. Sag versus radius for windows of various thickness.

Table 1: Quantities used in equation 1

Quantity		Units	Value
p	pressure loading	Pa	101324
a	window radius	mm	26
E	Young's modulus	Pa	7.6e+10
h	window thickness	mm	7.5
gamma	Poisson's ratio		0.26
diam/h			6.9
D	$Eh^3[12(1-\nu^2)]^{-1}$	Pa/m ³	2.9(10 ¹²)

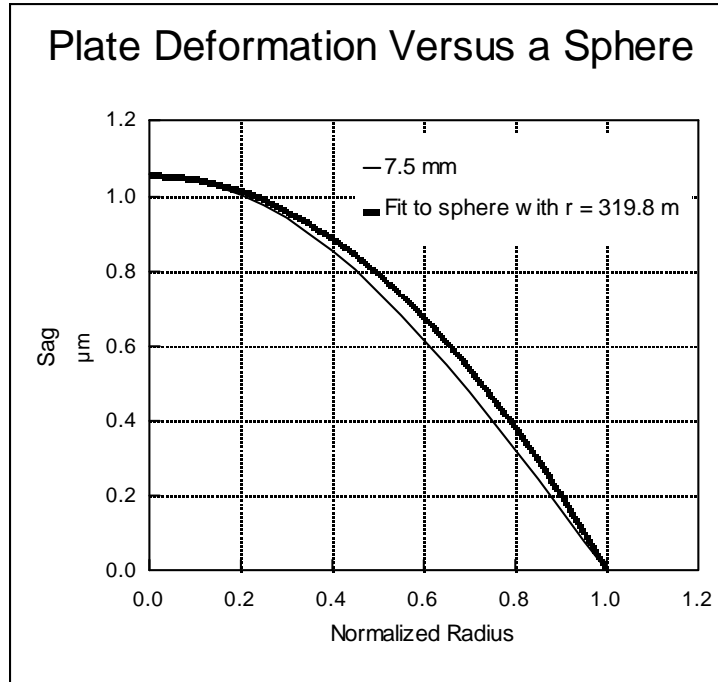


Figure 2. Plate deformation for a 7.5 mm CaF_2 window.

The window can be replaced by a negative meniscus in the optical design in order to estimate the effects on image performance. The radius for the meniscus is given by equation 2 where the sag is calculated at the center of the window, at zero normalized radius. For $h = 7.5$ mm, the sag is 1 : m and the radius is 338 meters. The large radius and small beam size at the window result in immeasurable induced aberrations at the slit focal plane. Figures 3 and 4 and show spot diagrams for a perfectly flat window and a negative meniscus window with $r = -1.0$ meters. The spot diagrams vary by field location in the vertical direction and by wavelength in the horizontal direction. The field points correspond to: (0,0), (230,-230), (230,230), (-230,230), and (-230,-230). Even for this smaller radius, the induced aberrations are nearly imperceptible.

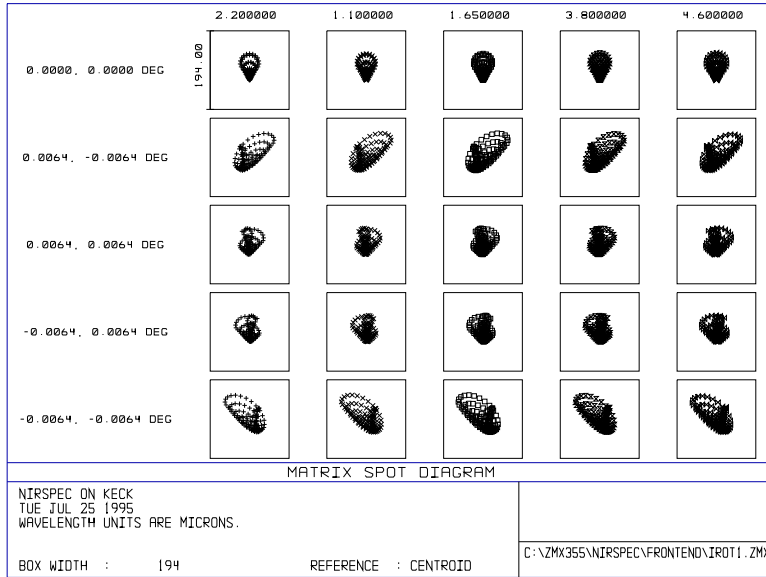


Figure 3. Spots for a perfectly flat window.

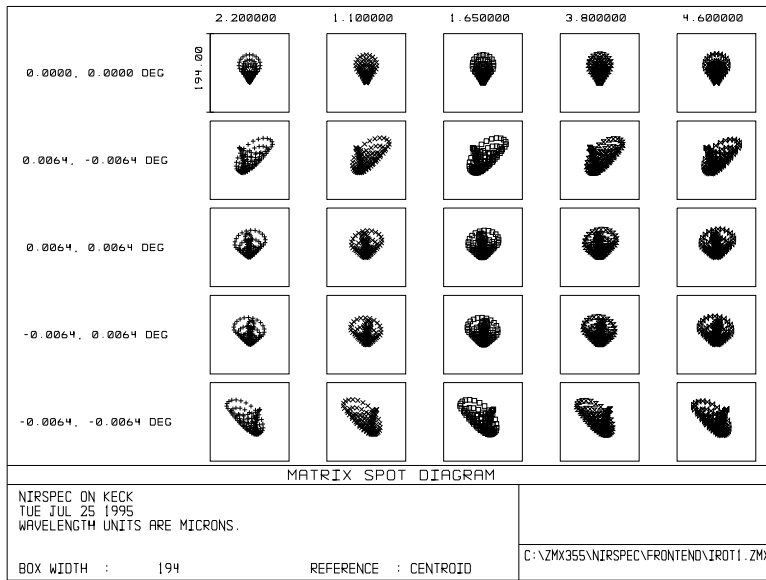


Figure 4. Spots for a negative meniscus window with $r = -1.0$.

2). Image shift and wander

Image shift describes the transverse shift of an image at the focal plane. This condition occurs when the optical axis of the input beam is decentered with respect to the optical axis of the image rotator, e.g. in the case that the dewar window is tilted. Image shift can be calculated for tilted, plane-parallel plates by using equation 3 from p. 98 of Smith's book. This assumes that the instrument is perfectly aligned with the telescope. The scaling factor $f_{\text{tele}}/f_{\text{fcon}}$ takes into account the demagnification to the slit focal plane. We can invert this equation to solve for $\theta_{t,\text{max}}$ in the case that $d = 1 \text{ pixels} = 75 \text{ : m}$ at the slit focal plane. Assuming a CaF_2 window and $h = 7.5 \text{ mm}$, we get $\theta_{t,\text{max}} = 1.45/(1.45-1) \times (0.075 \text{ mm}/7.5 \text{ mm}) \times 15/10 = 48 \text{ mrad} = 2.8^\circ$.

$$d = h \theta_t \frac{(n-1)}{n} \times \frac{f_{\text{fcon}}}{f_{\text{ftele}}},$$

where h = window thickness,
 θ_t = tilt angle,
 n = index of the window,
 f_{ftele} = f/number of telescope,
and f_{fcon} = f/number of the f-converter. (3)

Image wander describes the effect, at a focal plane, of an image spot rotating about an axis which is not coincident with the chief ray of the field point. This effect can be present in a system where there is image shift, and the object field is rotating. In NIRSPEC, object field rotation is compensated by an "image rotator," so that image points remain fixed even as the object field is rotating. However, when image shift is present, the images will rotate about the image rotator axis. The wander is along a circle with a radius equal to the image shift, and the wander rate is equal to twice the image rotator's rotation rate. This wandering effect is actually the troubling aspect of image shift. A shift could easily be taken out by moving the telescope until the object is in the slit. In fact, this has to happen for an observation anyway. The difficulty is that the image will then wander out of the slit if the dewar window is tilted beyond some critical angle. This tilt has identical effects whether it is about the x- or y-axis.

3). Pupil shift and wander

Pupil shift describes the transverse shift of the pupil image at the Lyot stop. This condition occurs when the input beams to the image rotator are not parallel to the optical axis of the collimator. Of course, the input beams corresponding to different field points on the sky cannot be telecentric in the strict sense, so each beam corresponding to an individual field point will form a pupil image having a particular shift. A ray trace to the Lyot stop, in fact, will show this effect in that rays from individual field points will not be strictly coincident for a given pupil point. This effect is not important for ideal alignments and element fabrication, but it can become important as the case deviates from ideal.

Figure 5 shows a side view of a ray trace where pupil shift is induced by a window with non-parallel surfaces. Figure 6 shows a close-up layout trace at the Lyot stop for the same design used to produce Figure 5. Notice that the ray pattern appears to be shifted downward with respect to the fixed cross-hair in the center of the stop. In this design, the first surface of the window is normal to the optical axis, but the second surface of the window is tilted at a 1° angle. The effect is that the nearly telecentric input beams are deviated so that the output beams are no longer parallel with the optical axis of the collimator. The pupil shift is given by equation 4. For NIRSPEC, $z = 60 \text{ mm} + 300 \text{ mm} = 360 \text{ mm}$ when the tilt is at the second surface of the dewar window. In this case, the pupil shift will be 2.8 mm for $\theta_{np} = 1^\circ$ and a CaF_2 window. As might be expected, there is also an appreciable amount of image shift, in this case equal to about 2 pixels. So, such a large amount of non-parallelism will cause the Lyot stop to partially occlude the beam and the images will shift, thus inducing image wander. We could invert equation 4 to calculate some maximum amount of non-parallelism, $\theta_{np,max}$, much like we inverted equation 3 to calculate $\theta_{t,max}$. However, we first have to determine what amount of pupil shift or image shift are acceptable. From the front-end bid packages, we can see that there is an allowance for 1 pixel of image wander and 1% pupil shift (267 : m). Using the Zemax model, I find an image shift of 1 pixel for $\theta_{np} = 0.15 = 9\text{N}$. For a 1% pupil shift, I get $\theta_{np} = 0.09 = 5\text{N}$, so, the non-parallelism requirement is set by pupil shift.

$$\text{pupil shift} = z \tan(\arcsin(n \sin \theta_{np}) - \theta_{np}), \quad (4)$$

where z = the distance between the tilted surface and the collimator
and θ_{np} = the tilt angle of the non-parallel surface.

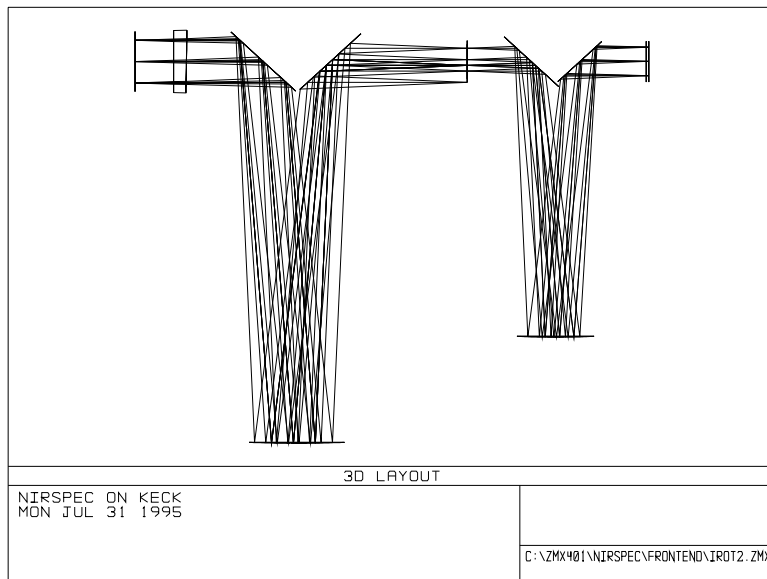


Figure 5. Side-view trace for front-end with a non-parallel window, $2_{hp} = 1^\circ$. Rays have been traced from 3 field points: center, and opposite corners of SCAM FOV.

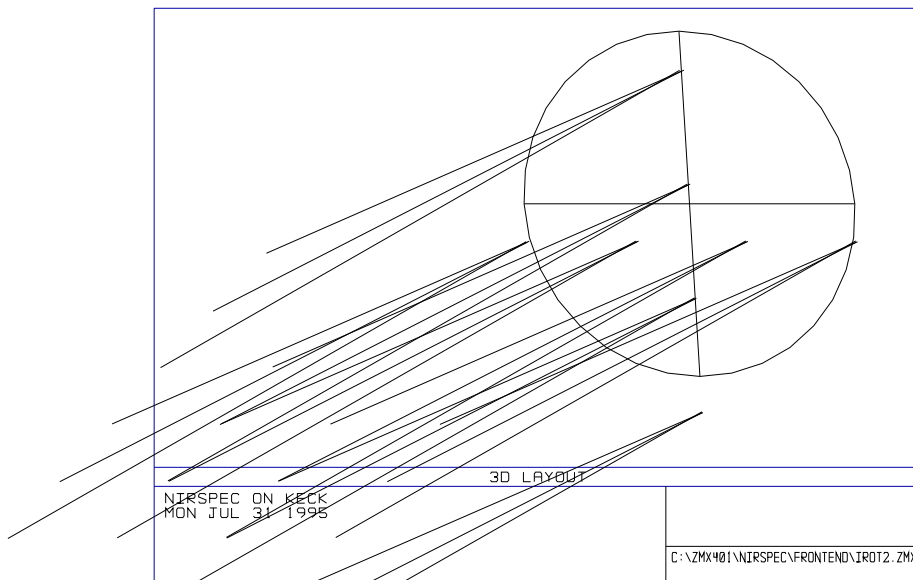


Figure 6. Layout-view trace at pupil plane of design shown in Figure 5. Rays have been traced through 8 pupil points.

4). Throughput

The transmission for uncoated CaF_2 is quite high, about 94% according to the Gemini optical design paper published in SPIE proceedings. An anti-reflection (AR) coated window will have even higher transmission (- 96% according to the NIRSPEC proposal); but a broadband coating kept flaking off the Gemini window. The coating on the outside surface of the window fell off, implying that humidity might have been the culprit. Janos claim that the faulty coating was due to a dirty manufacturing environment, but their reapplied coating also flaked off the window.

It appears that we have only a few options concerning the AR coating:

- 1). pursue more robust coatings with Janos
- 2). find other vendors who might be able to provide a robust coating
- 3). consider another substrate which can be coated

The last option can probably be ruled out, because an uncoated CaF_2 window has higher NIR transmission than just about any other AR-coated material. For example, an AR-coated ClearTran window has - 93% transmission, on average, between 1 and 5 μm .

5). Breakage and t_{\min}

According to the Optovac Catalog (p. 15), the minimum thickness for a window is shown in equation 5. Assuming an o-ring clamp, the appropriate values for a calcium fluoride (CaF_2) window are: $K = 0.8$ and $S = 5300$ psi. For a vacuum window, $p = 14.7$ psi. To take an example, i.e. for NIRSPEC, $D = 14.5$ mm X (23/15) X (15/10) X $\frac{1}{2}$ + 5 mm = 52 mm. So, $t_{\min} = 2.5$ mm, as shown in equation 6.

$$t_{\min} \approx \left(\frac{K \times p \times D^2}{S} \right)^{1/2}, \quad (5)$$

where $K =$ the safety factor,
 $p =$ pressure differential,
 $D =$ the unsupported diameter,
and $S =$ the apparent elastic limit.

$$t_{\min} \approx \left(\frac{0.8 \times 14.7 \text{ psi} \times (52 \text{ mm})^2}{5300 \text{ psi}} \right)^{1/2} = 2.5 \text{ mm}. \quad (6)$$

Given the clear diameter, D/t would be 21 if using t_{\min} as the window thickness. This is greater than D/t for the Gemini and KCAM windows ($D/t = 10$). In any case, t_{\min} is only a minimum specification for overcoming potential breakage. Another potential problem is that of surface deformation due to the pressure differential across the window.

Final Design

Although the window is one of the most simplistic optics in the instrument, some care has to be taken to make sure it performs in accordance with system requirements. The table below summarizes the discussion above by itemizing each performance consideration and associated physical tolerances on the opto-mechanical design and alignment procedure.

Table 2: Summary of design specifications for window

item	requirement	parameter	value
clearance	100% + 5 mm	D	52 mm
breakage		t	7.5 mm ^a
image wander	$r_{\text{wander}} < 0.1$ pixels	2_{p}	2°8
		2_{up}	5N

^aAdditional factor of 3 added for safety.